© Pol J Radiol 2022; 87: e430-e437
DOI: https://doi.org/10.5114/pjr.2022.118899

Received: 06.08.2021
Accepted: 13.12.2021
Published: 05.08.2022

Polish Journal of Radiology

http://www.polradiol.com

Original paper

The role of magnetic resonance imaging and magnetic resonance sialography in the evaluation of salivary sialolithiasis: radiologic-endoscopic correlation

Omneya Gamaleldin[1,A,B,D,E,F], Emad A. Magdy[2,A,B,D,E], Hesham Zoheir[1,A,B,D,E,F], Gihan Mohamed Shehata[3,C], Nermeen Elsebaie[1,A,B,D,E,F]

[1]Department of Diagnostic and Interventional Radiology, Alexandria Faculty of Medicine, Alexandria University, Egypt
[2]Department of Otorhinolaryngology-Head and Neck Surgery, Alexandria Faculty of Medicine, Alexandria University, Egypt
[3]Department of Medical Statistics and Biomedical Informatics, Medical Research Institute, Alexandria University, Egypt

Abstract

Purpose: To evaluate the role of magnetic resonance imaging (MRI) and MR sialography in salivary gland calculi in correlation with sialendoscopy.

Material and methods: In this prospective study, pre-therapeutic MRI was performed for patients with clinically suspected sialolithiasis. In addition, sialendoscopy with or without surgery was performed. The detectability, number, size, and location of calculi (distance of obstruction from the ostium and masseter line) and the condition of the main duct at MRI were reported. Agreement between the 2 readers was confirmed for all MRI findings. Data regarding the detectability, number, and size of calculi were correlated with endoscopy.

Results: There was excellent agreement between the 2 readers regarding the detection and number of calculi at MR sialography ($\kappa = 1$, $p < 0.001$). As regards MRI measurements, excellent interclass correlation was found between the 2 readers regarding size of calculi, distance of calculi from the ostium, and distance from the masseter line ($\kappa = 0.98, 0.98, 0.97$, respectively; $p < 0.001$). In correlation with sialendoscopy, MRI was false negative in 1 patient, and it missed 1 calculus in 3 patients with multiple calculi. There was no statistically significant difference between the size of calculi detected by MRI and true size of calculi retrieved by sialendoscopy.

Conclusion: MR sialography is an accurate modality for diagnosis of the presence, size, and location of sialolithiasis and offers accurate ductal mapping for sialendoscopists.

Key words: MR sialography, sialolithiasis, salivary gland, sialendoscopy.

Introduction

Obstructive salivary gland pathology is the most frequent non-neoplastic salivary gland disorder. Many causes are implicated including sialolithiasis, mucous plugs, ductal strictures, and foreign bodies. Sialolithiasis has been reported as the main cause of salivary obstructive disease and comprises more than 60-70% of all salivary duct obstructions. Sialolithiasis is estimated to affect 1% to 2% of the population [1]. Sialolithiasis is usually managed by conservative treatment; if unsuccessful, surgical excision of the involved salivary gland would be considered. However, sialadenectomy has the potential to cause injuries to the lingual and facial nerves as well as post-surgical complications, and therefore management of salivary duct obstruction has changed over the past years [2]. Sialendos-

Correspondence address:
Nermeen Elsebaie, Department of Diagnostic and Interventional Radiology, Alexandria Faculty of Medicine, Alexandria University, Egypt,
e-mail: nermeenmonsef@yahoo.com

Authors' contribution:
A Study design · **B** Data collection · **C** Statistical analysis · **D** Data interpretation · **E** Manuscript preparation · **F** Literature search · **G** Funds collection

copy is a relatively new procedure that allows endoscopic transluminal visualization of major salivary gland ducts, which can be both diagnostic and therapeutic [3]. Nowadays, sialendoscopy is considered a beneficial technique because it is less invasive and has a lower morbidity rate [4].

Imaging techniques available for investigation of salivary calculi before intervention include sonography, digital subtraction sialography, computed tomography (CT), and magnetic resonance (MR) sialography. While ultrasonography is usually the first line of diagnostics, it is highly operator dependent [5,6]. Sialography is considered the gold standard because it gives a clear image of the calculi and the duct morphology. However, it has the disadvantage of requiring cannulation of the punctum of the salivary duct, exposing the patient to a high dose of radiation and injection of contrast solution that can lead to a deeper displacement of the obstructing calculus. It is contraindicated in the acute setting due to the potential exacerbation of symptoms associated with infection [7]. Non-contrast CT of the neck can visualize salivary calculi because it is sensitive for the detection of calcifications; however, assessment of the glandular parenchyma and ductal dilatation are often lacking [8].

MR sialography is an increasingly popular diagnostic technique in which the patient's own salivary secretion is used as a natural contrast agent and which can be conducted quickly and without any complications. It provides noninvasive accurate visualization of the ductal system of major salivary glands, especially in cases that could prove to be difficult to examine by conventional sialography [9,10]. The aim of this study was to assess inter-reader agreement for the presence, number, size, and location of salivary gland calculi on magnetic resonance imaging (MRI) and MR sialography and compare MRI findings with sialendoscopy results. We have proposed certain MRI measurements for accurate localization of calculi, which could be relevant to the endoscopist and are likely to contribute to improved surgical outcomes.

Material and methods

Study design

This prospective study was approved by the review board of our institution, and written informed consent was obtained from all patients before initiation of all procedures. From June 2019 to March 2021, 40 consecutive patients with acute or recurrent postprandial salivary gland swelling and colicky pain were referred from the Department of Otorhinolaryngology for suspected salivary calculi. Our study included pre-therapeutic MRI to verify sialolithiasis and to provide detailed data about the location of calculi and ductal changes. In addition, sialendoscopy with or without surgery was performed. MRI was not feasible in 1 patient because of claustrophobia, and sialendoscopy failed in 3 patients. These patients were excluded from the study. The other 36 patients (26 female, 10 male; mean age 38.3 years) formed the study group.

Magnetic resonance imaging

MRI examination was performed with a 3.0 T MR imaging system (Ingenia, Philips Medical Systems, Best, Netherlands) or a 1.5 T MR imaging system (Achieva, Philips Medical Systems, Best, Netherlands). A 16-channel sense neurovascular head and neck coil was used. MR images were obtained with spin-echo sequences on the 3T system as follows: T1-weighted (TR/TE = 500 ms/14 ms), T2-weighted (TR/TE = 2600 ms /80 ms), and short inversion time–inversion recovery (SITR) (TR/TE = 2000 ms/14 ms, time of inversion [TI] = 160 ms). Axial sections were obtained with a 4 mm slice thickness without interslice gap and 256 × 256 acquisition matrix for all sequences. For MR sialography, a T2W-3D-DRIVE sequence was used, and the imaging parameters were as follows: TR/TE = 2000 ms/200 ms, slice thickness = 0.5 mm. The sequence took approximately 2 min 20 sec. Images were obtained in the axial plane and reconstructed in sagittal and coronal planes on the workstation. On the 1.5 T system the same sequences were performed using the following parameters: T1-weighted (TR/TE = 400 ms/17 ms), T2-weighted (TR/TE = 2660 ms /80 ms), and short inversion time–inversion recovery (SITR) (TR/TE = 1800 ms/30 ms, time of inversion [TI] = 150 ms). For MR sialography a T2W-3D-DRIVE sequence was used, and the imaging parameters were as follows: TR/TE = 1500 ms/400 ms, slice thickness = 0.6 mm. The sequence took approximately 2 min 32 sec.

Image analysis

The MR images were reviewed at a workstation by 2 radiologists (GO, EN) with 12 and 11 years' experience in MR imaging, respectively. They independently reviewed the images blinded to patient data and final diagnosis. The source images, together with the maximum-intensity-projection and multiplanar reformat reconstructions, were analysed. The reviewers recorded the presence, number, size, and location of calculi. Calculi were diagnosed when round, ovoid, or irregularly shaped signal voids were identified within or immediately next to a dilated or nondilated salivary duct. They reported whether one or multiple calculi were present within the ductal system. The size of each calculus was expressed as the maximal diameter.

The locations of calculi were specified objectively by measuring the distance of calculus from the ostium on T2-weighted images. In the case of the submandibular gland, it was measured from the anterior edge of the genioglossus muscle in the midline to the site of the calculus (Figure 1). In the case of the parotid gland, it was measured from the outer cortical border of the maxilla opposite the upper

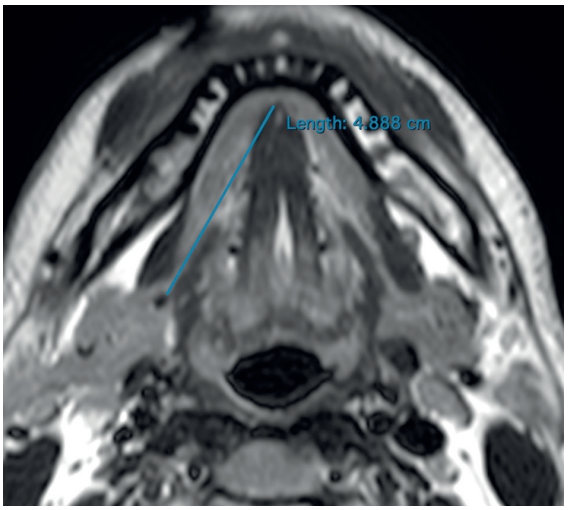

Figure 1. Measurement of the site of right hilar submandibular gland calculus in T2-weighted sequence from the anterior edge of genioglossus muscle in the midline to the anterior border of the signal void calculus

Figure 2. Measurement of left parotid duct calculus from the ostium. It is measured from the outer cortical border of maxilla opposite upper second molar tooth to the curve of masseter muscle (masseteric line) and then from the masseteric line to the anterior edge of the signal void calculus

second molar tooth to the anterior border of the masseter muscle (masseteric line) and then from the masseter line to the site of the calculus (Figure 2). Additionally, for parotid duct calculi, the location of the calculus, whether anterior or posterior, to the masseteric line was reported. Then, for calculi posterior to the masseteric line, the distance between the calculus and the masseteric line was also measured.

The condition of the duct was assessed at both T2-weighted and MR sialography images. The diameter of the duct was measured distal to calculi, and wall thickening was assessed on T2-weighted and STIR images. If the duct was less than 2 mm in diameter, it was considered collapsed. If the duct was less than 2 mm in diameter with thickened wall or if there was abrupt transition from ductal dilatation to tapered appearance of the salivary ducts, duct stricture was suggested. Upstream duct dilatation was also detected and measured.

Sialendoscopy

Sialendoscopy for calculus retrieval was performed within 2 weeks of the MRI by an otorhinolaryngology surgeon (ME) with 10 years' experience in the procedure. Sialendoscopy was performed under general anaesthesia using semi-rigid Marchal All-in-one miniature 1.3 mm or 1.6 mm diameter endoscopes with working and flushing channels (Karl Storz GmbH, Tuttlingen, Germany). The endoscope was introduced into the gland duct following serial dilation of either the submandibular or parotid duct papilla. The presence of calculi in the ductal system of the gland was then examined. Sialolithiasis management manoeuvres included sialendoscopy and basket extraction, combined sialendoscopy and open approaches, microscopic-assisted intraoral sialolithotomy, and simple intraoral duct cut down.

Statistical analysis

Statistical analysis was performed using SPSS software (version 21, IBM). Descriptive statistics were used to record calculus characteristics (size, distance from ostium, and distance from masseter line). Kappa statistics were calculated for agreement between the 2 readers in calculus detection. Reliability analysis was done by using the intraclass correlation coefficient (ICC) to test the agreement between 2 readers of MRI measurements. Inter-reader agreement was defined as follows: a κ/ICC values of 0-0.20, poor agreement; 0.21-0.40, fair; 0.41-0.60, moderate; 0.61-0.80, good; and 0.81-1.00, excellent. A 95% confidence interval (CI) for the κ/ICC values was also reported. Bland-Altman analysis was used to compare the MRI measurements by the 2 readers and to determine the interobserver agreement between them. The calculus size measured at MRI and after endoscopic extraction was compared using the *t*-test.

Results

The inclusion criteria yielded 36 patients. There were 26 female (72.2%) and 10 male patients (27.8%) with a mean age of 38.3 ± 14 years (range 4-64 years). The presenting symptoms were recurrent postprandial colicky pain (n = 17) and recurrent postprandial salivary gland swelling (n = 19). Sialolithiasis was present in the submandibular system in 21 patients and in the parotid system in 15 patients.

Magnetic resonance imaging findings

Calculus characteristics (detection, size, and location)

Forty-nine calculi were identified on MR sialography. Thirty-one of the calculi were in the submandibular system and 18 calculi were in the parotid system. A single calculus

was present in 22 patients, and multiple calculi were present in 13 patients. There was excellent agreement between the 2 readers regarding the presence and number of calculi ($\kappa = 1$, $p < 0.001$). The calculi ranged in size from 1.5 to 19 mm, with a mean diameter of 6.1 ± 2.9 mm and 6 ± 2.9 mm for the first and the second readers, respectively. The first reader reported 28 calculi to be less than 6 mm, compared to 27 calculi reported by the second reader. There was excellent interclass correlation between the 2 readers regarding the size of calculi ($\kappa = 0.98$, $p < 0.001$).

The distance of the calculus from ostium ranged from 0.8 to 6.7 cm with a mean of 3.8 ± 1.6 cm for the first reader and from 0.7 to 7 cm with a mean of 3.8 ± 1.5 cm for the second reader. Five calculi were located at the ostium. There was excellent interclass correlation between the 2 readers ($\kappa = 0.98$, $p < 0.001$). In the parotid system, for calculi located behind the masseter line, the distance of the calculus from the masseter line ranged from 0.7 to 5.2 cm with a mean of 2.9 ± 1.5 cm and from 0.6 to 5.3 cm with a mean value of 3 ± 1.5 cm for the first and second readers, respectively. There was excellent interclass correlation between the 2 readers regarding the distance of the calculus from the ostium calculi ($\kappa = 0.98$, $p < 0.001$) and from the masseter line ($\kappa = 0.97$, $p < 0.001$). Data of interobserver agreement regarding all MRI measurements are shown in Table 1 and illustrated by Bland-Altman plot (Figure 3).

Condition of the duct

Duct stricture was suggested diagnosis in 5 patients (5/36); it involved the parotid duct in 3 patients and the submandibular duct in 2 patients. Stenosis was localized at the level

Table 1. Interobserver agreement regarding magnetic resonance imaging (MRI) findings

MRI findings	R1	R2	Kappa/ICC	95% CI
Number of detected calculi	49	49	1	1
Size, range (median); mean ± SD, mm	1.5-19.0 (5.8); 6.1 ± 2.9	1.5-19.0 (5.5); 6.0 ± 2.9	0.98	0.969-0.990
Distance from ostium, range (median); mean ± SD, cm	0.8-6.7 (4); 3.8 ± 1.6	0.7-7.0 (4.0); 3.8 ± 1.5	0.98	0.974-0.992
Distance from masseter line, range (median); mean ± SD, cm	0.7-5.2 (3.1); 2.9 ± 1.5	0.6-5.3 (3.5); 3.0 ± 1.5	0.97	0.917-0.991

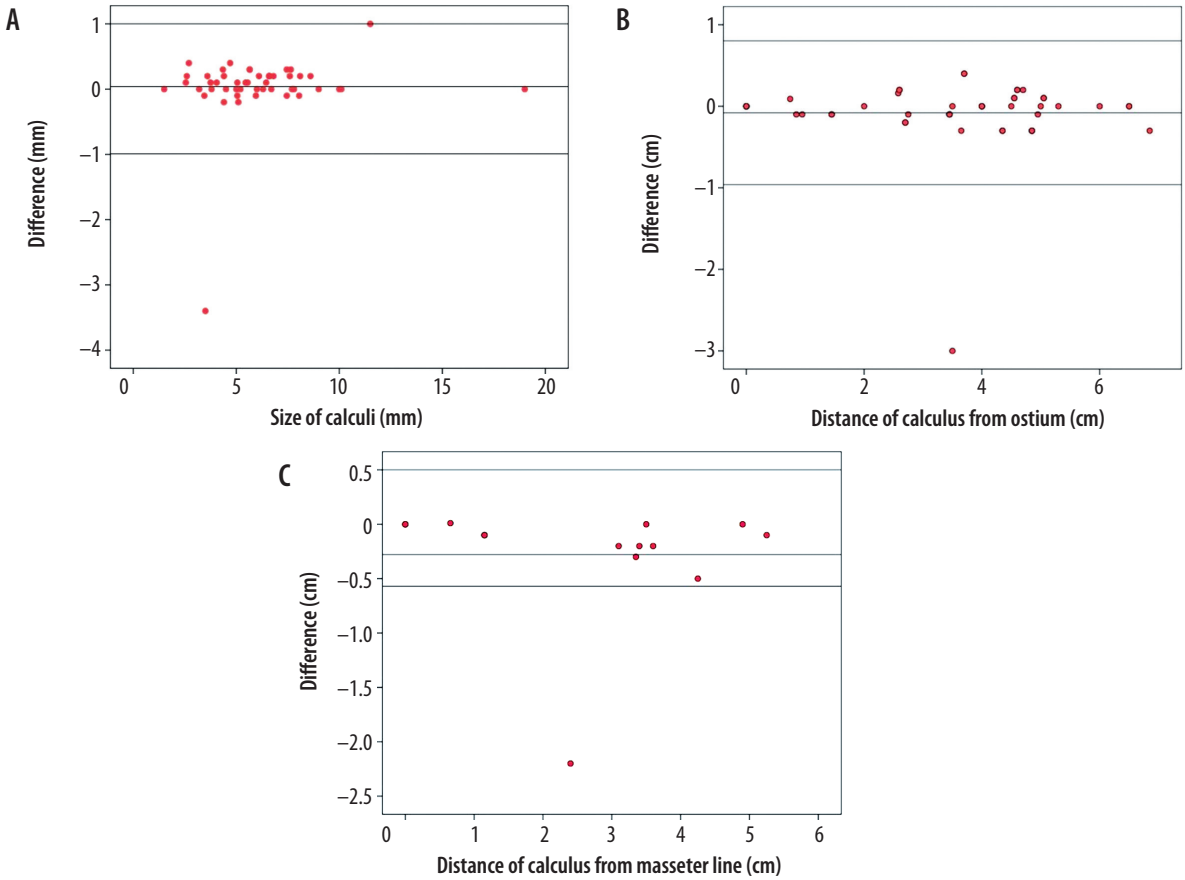

Figure 3. Magnetic resonance imaging measurements by 2 readers. Bland-Altman plots of interobserver agreement for size of calculus **(A)**, distance of calculus from ostium **(B)**, and distance of calculus from masseter line **(C)** show that almost all values lie within limits of agreement. Data points represent individual stones; solid lines represent mean difference

of the main salivary ducts. The location of stricture was distal in 3 cases and in the middle of the Stensen duct in 2 cases. In all glands stenosis was associated with upstream ductal dilatation at MR sialography.

Correlation with endoscopic findings regarding detectability, number, and size of calculi

MR sialography detected 49 calculi compared to 53 calculi retrieved at endoscopy; 4 calculi were missed in 4 patients. MRI was false negative in 1 patient, and it missed 1 calculus in 3 patients with multiple calculi. Three of the missed calculi were in the submandibular gland, 2 were located in the proximal portion of the submandibular duct (Figure 4), and 1 was just behind the ostium; they measured less than 3 mm as measured after endoscopic extraction. In the fourth patient, 2 parotid duct calculi were found by endoscope, which were perceived at MR sialography as a single large calculus (Figure 5). The size of calculi detected at MR sialography ranged between 1.5 and 19 mm, with a mean of 6.1 ± 2.9 mm. After endoscopy, the actual size of the retrieved calculi ranged from 1.5 to 17 mm with a mean diameter of 5.9 ± 2.9 mm. There was no significant difference between size measured at MR sialography and extracted calculi size ($p = 0.3$).

Endoscopic intervention

Based on clinical examination and MRI findings, the surgical procedure was chosen. For submandibular calculi ($n = 34$), sialendoscopy with basket extraction was done for 12 calculi (in nine patients); all of these calculi were less than 6 mm (range 2-5.8 mm). Endoscopic assisted lithotomy was done for 20 calculi (in 10 patients); 8 patients had more than 1 calculus, at least 1 of these calculi was more than 6 mm (range, 6.2-12 mm), and 2 patients had single calculus exceeding 6 mm. Simple intraoral cut down was done for 2 calculi (in 2 patients) located at the ostium; their sizes were 6.5 and 19 mm.

For calculi in the parotid system ($n = 19$), sialendoscopy with basket extraction was done for 10 calculi (in 8 patients), all were less than 6 mm. Regarding their location, 3 calculi were anterior to the masseter line, 2 were along the masseter line, and 5 were posterior to the masseter line, at a distance less than 3 cm (range 0.7-3 cm). Combined endoscopic and open surgical external approach was done for 7 calculi (in 6 patients), calculi ranged from 4 to 9 mm and were located posterior to the masseter line at a distance of more than 3 cm (range 3.5-5.2 cm). A combined endoscopic and open surgical intraoral approach was performed in 1 patient with 2 calculi anterior

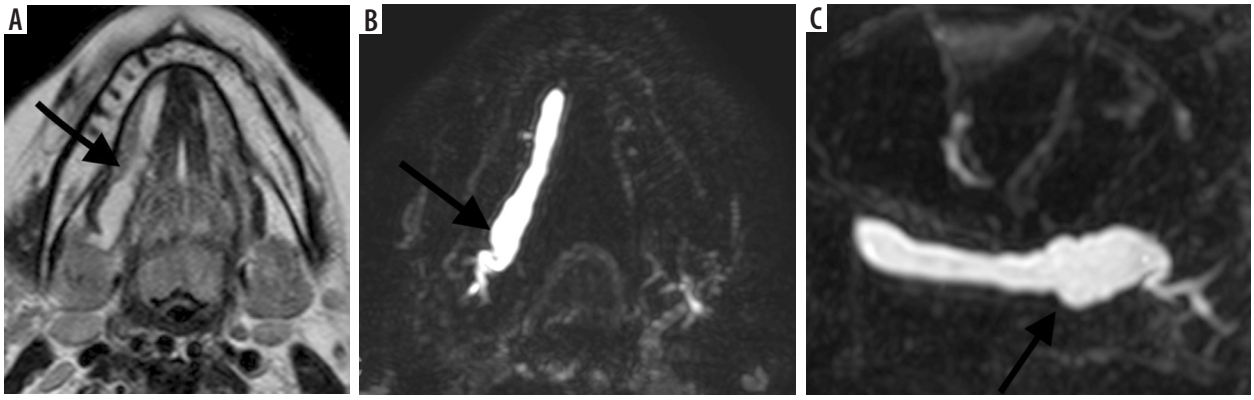

Figure 4. A, B) Axial and sagittal magnetic resonance sialography images revealed dilatation of Wharton's duct along its whole length with abrupt change in calibre at its distal end and rounding of the duct at the ostium indicating distal stricture. **C)** A hilar calculus measuring 2 mm was detected by sialendoscopy, and it was removed after dilation of the stricture

Figure 5. A) Sagittal magnetic resonance sialography image showing single large calculus measuring 7.8 mm (black arrow). **B)** Axial T2-weighted image showed the signal void calculus inside the dilated main duct (black arrow). Considering calculus size (more than 6 mm) and distal location, just anterior to the masseter line, combined sialendoscopy and intraoral approach was done. **C)** Endoscopy revealed 2 calculi measuring 6 and 2 mm

to the masseter line (size more than 6 mm). Two patients were treated by endoscopic serial dilatation followed by basket extraction of calculi. Combined endoscopic and surgical management was done in 3 patients because the calculi were larger than 8 mm and located behind a stenosis that could not be dilated (Figure 6). All the patients' symptoms improved after surgery, and no further surgery was needed at the time of preparing this article.

Discussion

In our study, we performed MR sialography using a T2W-3D-DRIVE sequence in addition to T2WI and STIR sequences in patients with sialolithiasis. There was excellent agreement between the 2 readers regarding detectability and number of calculi ($\kappa = 1$; $p < 0.001$). As regards MRI measurements, excellent interclass correlation was found between the 2 readers regarding the size of calculi, distance of the calculi from the ostium, and the distance from the masseter line ($\kappa = 0.98, 0.98, 0.97$, respectively; $p < 0.001$). MRI was false negative in one patient, and it missed 1 calculus in 3 patients with multiple calculi. The sensitivity of MR sialography has previously been reported to be 91% [10]. In another study, the sensitivity of MR sialography was 73% and specificity was 96%. They used a 3-dimensional CISS sequence on a 1.5 T scanner [11].

Sialolithiasis is the most common benign disorder of the salivary glands. Eighty to ninety per cent of calculi are found in the submandibular system, due to the more viscous, alkaline saliva and upward course of the duct promoting stasis. Parotid calculi account for only 5-10% of cases, mostly due to the less steep course of the Stensen duct, serous composition of secretions, and lower concentration of sequestered calcium [10,12]. In our study, about 64% of all calculi detected after endoscopic management were located in the submandibular system compared to 36% in the parotid system; this difference in comparison to the rates published in the literature may be because we only imaged symptomatic patients who required intervention, while patients with small calculi may be asymptomatic. The peak incidence of sialolithiasis occurs from 30 to 60 years of age [13]. The mean patient age in our study was 38.3 years, and there was a female predominance of 72.2%, correlating with that in previously published studies [1,10]. Three paediatric patients were included in our study. Childhood sialolithiasis is quite rare, accounting for about 3-5% of all salivary calculi [14,15].

The size and location of the calculus as well as the presence of strictures all have a significant impact on management. Most salivary calculi range between 3 and 7 mm in size; they can grow to large sizes (8 mm) but rarely grow to over 15 mm, at which point they are defined as giant sialoliths [16]. Calculus size is very important; calculi up to 4 mm in the submandibular gland and less than 3 mm in the parotid gland can be removed by basket. Calculi less than 6 mm with regular contour can be extracted simply using the basket if in an accessible location. In moderately sized calculi 6-8 mm in diameter sialendoscopy-assisted surgery can be performed if fragmentation tools are not available. Calculi larger than 8 mm will require a combined approach [17,18]. In our study, the mean diameter of calculi was 6.1 ± 2.9 mm. Sialendoscopy and basket extraction was performed for 22 calculi; their size was less than or equal to 6 mm; 10 of these calculi were in the parotid and 12 in the submandibular ducts.

Besides the size, the location of calculus also has a remarkable influence on the therapeutic procedure. In the submandibular system, calculi located at the distal and middle thirds of Wharton's duct can be easily removed using sialendoscopy. The removal of calculi in the proximal third of Wharton's duct, at the hilum or intraglandular area, particularly if more than 6 mm, is more challenging. In such circumstances, endoscopic assisted lithotomy can be adopted [19]. Li *et al.* [20] successfully performed sialendoscopy-assisted trans-oral incisions in 20 patients with larger and proximal location of stones in Wharton's duct, with gland preservation and no recurrence of symptoms. In our study, endoscopic assisted lithotomy was performed for 20 calculi (in 10 patients); 8 patients had more than 1 calculus, at least 1 of these calculi was more than 6 mm, and the other 2 patients each had a single calculus exceeded 6 mm. The calculi were located proximally within Wharton's duct, precisely, at a distance of more 3 cm from the ostium as measured at MRI. Xiao *et al.* [21] used the same procedure for 8 patients with proximal submandibular calculi, all exceeding 6 mm.

In the parotid system, the location of calculi in relation to the masseter line will change the surgical procedure. Calculi located anterior to the masseter line can be accessed through an intraoral approach, unlike calculi near the hilum, which are managed using a pre-auricular method [22,23]. In our study, a combined endoscopic and open surgical external approach was performed for calculi located posterior to the masseter line at a distance 3 cm or more as measured at MRI. Combined endoscopic and open surgical intraoral approach was performed for calculi anterior to the masseteric line (size more than 6 mm). Calculi located at or posterior to the masseter line at a distance of less than 3 cm (size less than 6 mm) were amenable to endoscopic extraction. Saga-Gutierrez *et al.* [24] used a combined endoscopic and open surgical intraoral approach in 8 patients in his study, with calculi located anterior to the masseter line, and the mean size of the calculi was 9.6 mm. Kiringoda *et al.* [25] in their study found that calculi visualized on sialendoscopy were significantly closer to the anterior border of the masseter muscle (masseter line) compared to calculi that were not seen on sialendoscopy.

Ductal stenosis is the second most common cause of obstructive sialadenitis, with frequent parotid gland involvement. Around 70-75% of stenoses are located in the parotid and 25-30% are found in the submandibular duct system.

Figure 6. **A)** Axial T2-weighted image showed signal void calculus measuring 5.8 mm (black arrow), the calculus was located 3.5 cm behind the masseter line. **B)** Sagittal MR sialography image showed stricture of the duct distal to and surrounding the calculus with moderate upstream duct dilatation. **C)** Axial STIR sequence showed the duct distal to and surrounding the calculus (white arrow) narrowed with thickened wall. Combined sialendoscopy and open external approach was done; the extracted calculus measured 6 mm

Stenoses are associated with sialolithiasis in over 15% of cases in the parotid gland and in 2-5% of cases in the submandibular glands. The presence of a stricture distal from the calculus is an important cause of failed endoscopy. In addition, if calculus fragmentation is used, it prevents fragments moving downstream, and if surgery is deployed, it can lead to sialoceles. MR sialography can display the duct diameter in its actual value, unlike conventional sialography in which administration of a contrast agent increases the lumen pressure and makes the diameter look greater than it actually is [26,27]. Obstructive sialadenitis due to combined calculi and duct stricture was found in 5 patients in our study; 3 in the parotid duct and 2 in the submandibular duct. Similar to Kopec *et al.* [28], we also found that stenoses of the distal and middle parts of the duct were more common.

When the commonly used MRI sequences, T2WI and STIR, are combined with 3D-DRIVE technique, it improves the detectability of salivary calculi, their number, and size [29,30]. Additionally, proper assessment of location of the calculus, distance from the ostium, and distance from the masseter line (in parotid calculi located behind the masseter line) as well as the condition of the duct distal to calculi, allow the endoscopist to decide on a suitable management plan [20,31]. Preoperative evaluation of the precise location of calculi would minimize the risk of failure. In our opinion, this is the first study that has used specific MRI measurements for localization of calculi and has assessed their role in patient management.

Our study has some limitations. First, the limited number of patients. Second, comparison with other imaging techniques to assess the difference in sensitivity of detection of calculi was not done; we focused on MRI findings in correlation with endoscopic data as a reference.

Conclusions

MR sialography is an accurate non-invasive diagnostic tool in patients suspected of having sialolithiasis. MR sialography can reduce the need for diagnostic endoscopies and limit endoscopy to therapeutic approaches, and thus might be cost effective for patients and obviate unnecessary interventions. MR sialography is an effective tool for diagnosis of the presence, size, and location of sialolithiasis, and it offers accurate ductal mapping for endoscopists.

Conflicts of interest

The authors report no conflict of interest.

References

1. Schrøder SA, Andersson M, Wohlfahrt J, et al. Incidence of sialolithiasis in Denmark: a nationwide population-based register study. Eur Arch Otorhinolaryngol 2017; 274: 1975-1981.
2. Schapher, M., Mantsopoulos, K., Messbacher, et al. Transoral submandibulotomy for deep hilar submandibular gland sialolithiasis. Laryngoscope 2017; 127: 2038-2044.
3. Rasmussen ER, Lykke E, Wagner N, et al. The introduction of sialendoscopy has significantly contributed to a decreased number of excised salivary glands in Denmark. Eur Arch Otorhinolaryngol 2016; 273: 2223-2230.
4. Pulickal GG, Singh D, Lohan R, et al. Dual-source dual-energy CT in submandibular sialolithiasis: reliability and radiation burden. AJR Am J Roentgenol 2019; 213: 1291-1296.
5. Thomas WW, Douglas JE, Rassekh CH. Accuracy of ultrasonography and computed tomography in the evaluation of patients undergoing sialendoscopy for sialolithiasis. Otolaryngol Head Neck Surg 2017; 156: 834-839.
6. Terraz S, Poletti PA, Dulguerov P, et al. How reliable is sonography in the assessment of sialolithiasis. AJR Am J Roentgenol 2013; 201: W104-109.
7. Ugga L, Ravanelli M, Pallottino AA, et al. Diagnostic work-up in obstructive and inflammatory salivary gland disorders. Acta Otorhinolaryngol Ital 2017; 37: 83-93.
8. Pulickal GG, Singh D, Lohan R, et al. Dual-source dual-energy CT in submandibular sialolithiasis: reliability and radiation burden. AJR Am J Roentgenol 2019; 213: 1291-1296.
9. Tanaka T, Oda M, Wakasugi-Sato N, et al. First report of sublingual gland ducts: visualization by dynamic MR Sialography and its clinical application. J Clin Med 2020; 9: 3676.
10. Purcell YM, Kavanagh RG, Cahalane AM, et al. The diagnostic accuracy of contrast-enhanced CT of the neck for the investigation of sialolithiasis. AJNR Am J Neuroradiol 2017; 38: 2161-2166.
11. Chellathurai A, Gnanasigamani S, Kumaresan S, et al. MR sialography and conventional sialography in salivary gland and duct pathologies: a comparative study. J Evolution Med Dent Sci 2016; 5: 3367-3372.
12. Abdel Razek AAK, Mukherji S. Imaging of sialadenitis. Neuroradiol J 2017; 30: 205-215.
13. Ogura I, Sasaki Y, Oda T, et al. Magnetic resonance sialography and salivary gland scintigraphy of parotid glands in Sjogren's syndrome. Chin J Dent Res 2018; 21: 63-68.
14. Capaccio P, Canzi P, Gaffuri M, et al. Modern management of paediatric obstructive salivary disorders: long-term clinical experience. Acta Otorhinolaryngol Ital 2017; 37: 160-167.
15. Schwarz Y, Bezdjian A, Daniel SJ. Sialendoscopy in treating pediatric salivary gland disorders: a systematic review. Eur Arch Otorhinolaryngol 2018; 275: 347-356.
16. Kim YM, Choi JS. Sialolith: how big? Ear Nose Throat J 2020; 99: 70-71.
17. Kroll T, Sharma SJ, Kähling C, et al. Sialendoscopy. Laryngorhinootologie 2015; 94: 292-293.
18. Costan VV, Ciocan-Pendefunda CC, Sulea D, et al. Use of cone-beam computed tomography in performing submandibular sialolithotomy. J Oral Maxillofac Surg 2019; 77: 1656.e1-1656.
19. Fabie JE, Kompelli AR, Naylor TM, et al. Gland-preserving surgery for salivary stones and the utility of sialendoscopes. Head Neck 2019; 41: 1320-1327.
20. Li J, Xu XY, Lu ZW, et al. Sialendoscopy-assisted intraoral incision approach for the treatment of posterior Wharton's duct stones: our experience and outcomes. Videosurgery Miniinv 2021; 16: 249-255.
21. Xiao JQ, Sun HJ, Qiao QH, et al. Evaluation of sialendoscopy-assisted treatment of submandibular gland stones. J Oral Maxillofac Surg 2017; 75: 309-316.
22. Saga-Gutierrez C, Chiesa-Estomba CM, Larruscain E, et al. Sialendoscopy assisted transoral approach for parotid gland lithiasis. Eur Arch Otorhinolaryngol 2021; 278: 567-571.
23. Roland LT, Skillington SA, Ogden MA. Sialendoscopy-assisted transfacial removal of parotid sialoliths: a systematic review and meta-analysis. Laryngoscope 2017; 127: 2510-2516.
24. Saga-Gutierrez C, Chiesa-Estomba CM, Larruscain E, et al. Sialendoscopy-assisted transoral approach for parotid gland lithiasis.Eur Arch Otorhinolaryngol 2021; 278: 567-571.
25. Kiringoda R, Eisele DW, Chang JL. Comparison of parotid imaging characteristics and sialendoscopic findings in obstructive salivary disorders. Laryngoscope 2014; 124: 2696-2701.
26. Koch M, Iro H. Salivary duct stenosis: diagnosis and treatment. Acta Otorhinolaryngol Ital 2017; 37: 132-141.
27. Carta F, Farneti P, Cantore S, et al. Sialendoscopy for salivary stones: principles, technical skills and therapeutic experience. Acta Otorhinolaryngol Ital 2017; 37: 102-112.
28. Kopeć T, Szyfter W, Wierzbicka M, et al. Stenoses of the salivary ducts-sialendoscopy based diagnosis and treatment. Br J Oral Maxillofac Surg 2013; 51: e174-177.
29. Gadodia A, Seith A, Sharma R, et al. Magnetic resonance sialography using CISS and HASTE sequences in inflammatory salivary gland diseases: comparison with digital sialography. Acta Radiol 2010; 5: 156-163.
30. Koontz NA, Kralik SF, Fritsch MH, et al. MR sialography: a pictorial review. Neurographics 2014; 4: 142-157.
31. Hills AJ, Holden AM, McGurk M. Sialendoscopy-assisted transfacial removal of parotid calculi. Acta Otorhinolaryngol Ital 2017; 37: 128-131.